Citation
Ha, N.S. and Marundrury, S.S. and Pham, T.M. and Pournasiri, E. and Shi, F. and Hao, H. 2022. Effect of grounded blast furnace slag and rice husk ash on performance of ultra-high-performance concrete (UHPC) subjected to impact loading. Construction and Building Materials. 329: ARTN 127213. http://doi.org/10.1016/j.conbuildmat.2022.127213

Effect of Grounded Blast Furnace Slag and Rice Husk Ash on Performance of Ultra-High-Performance Concrete (UHPC) Subjected to Impact Loading

Ngoc San Ha, Siga S. Marundrury, Thong M. Pham*, Emad Pournasiri, Feng Shi, Hong Hao*

Center for Infrastructural Monitoring and Protection, School of Civil and Mechanical Engineering, Curtin University, Kent Street, Bentley, WA 6102, Australia

*Corresponding author: thong.pham@curtin.edu.au; hong.hao@curtin.edu.au

Abstract

This paper investigates the effect of using alternative cementitious constituents on the compressive performance of Ultra-High-Performance Concrete (UHPC) for both static and dynamic conditions. The grounded blast furnace slag (GBFS) and rice husk ash (RHA) with different portions were used to replace 30% ordinary Portland cement (OPC) of a reference mix (UHPC-R1). Two alternative UHPC mixes including an UHPC mix with 30% GBFS mix (UHPC-AC1) and an UHPC mix with 15% GBFS and 15% RHA mix (UHPC-AC2) were considered. The quasi-static compressive strength and dynamic compressive strength of the proposed UHPC mixes were then determined using a compression testing machine and a Split Hopkinson Pressure Bar, respectively. The results indicated that UHPC-AC1 and UHPC-AC2 yielded a comparable performance compared to the reference mix UHPC-R1. In particular, the static compressive strength of UHPC-AC1 and UHPC-AC2 mixes were found to only be 5% and 10% less than those of the UHPC-R1 mix, respectively. In addition, the study also found that UHPC-AC1 and UHPC-AC2 achieved a similar dynamic compressive strength compared to the UHPC-R1, and the compressive strength of UHPC-AC1 and UHPC-AC2 were not strain rate sensitive. For the environmental aspect, UHPC-AC1 and UHPC-AC2 have a lower embedded CO_2 emission index compared to the reference UHPC-R1.

Keywords: UHPC; Grounded blast furnace slag (GBFS); Rice husk ash (RHA); Embodied carbon dioxide (e-CO2); Dynamic compressive performance.

1. Introduction

Ultra-high performance concrete (UHPC) has attracted great attention from civil engineering society due to its excellent mechanical and durability properties, less associated materials and lower installation and labour costs. An UHPC mixture commonly consists of cement, silica fume (SF), quartz powder, sand, superplasticizer (SP), water and steel fibre. In UHPC, fine aggregates like quartz sand were used instead of the coarse aggregates to reduce the weaknesses of the interfacial transition zone (ITZ) between the cementitious matrix and aggregates and more uniform stress flow. Meanwhile, SF with a finer particle size and spherical shape was added to UHPC to improve its performance by filling voids between coarser particles. Chan and Chu [1] recommended SF dosages of 20–30% of the total binders to achieve optimal strength properties of UHPC. Besides, an UHPC mixture also requires a very low water/binder ratio (*w/b*) with an optimal value of 0.13–0.20 as suggested by previous studies [2-4]. Wille, et al. [5] reported that UHPC can achieve a compressive strength higher than 150 MPa with the *w/b* ratio of 0.25. In addition, steel fibres are commonly added to ensure high ductility of UHPC and increase the energy absorption of the concrete [6, 7]. For an economical and workable UHPC mixture design, 2 % volume fraction of steel fibres was recommended [4]. Similar to normal concrete (NC) and high-performance concrete (HPC), cement plays a key role in the binding ability and performance of UHPC. UHPC uses a relatively high proportion of cement content as compared to NC and HPC [8]. It was observed that the compressive strength of UHPC increased first with the cement content, but decreased when the cement content was over the optimal content around 1,700 kg/m^3, due to limited participation of finer aggregates [9]. The UHPC

Although UHPC exhibits many excellent characteristics, its wider use in the construction industry is limited due to the relatively high initial cost. Due to incorporating many components as mentioned above, the manufacturing cost of UHPC is much higher than that of NC [10]. However, ongoing research and investigations are filling knowledge gaps to produce innovative UHPC with lower initial costs. Another concern of UHPC is that it used a large portion of cement that is a virgin ingredient that requires intensive energy for production. It therefore has bad impact to the environment. Abdulkareem, et al. [11] found that the common amount of ordinary Portland cement (OPC) per cubic metre for the majority of UHPC mixes was generally around 1,100 kg/m^3, which is nearly triple the amount in ordinary concrete [11]. It is well-known that the OPC contributed to nearly 8% of global CO_2 emissions [12]. Therefore, to reduce the negative environmental impact of CO_2 caused by producing UHPC, appropriate alternative cementitious constituents are sought to replace OPC without scarifying the UHPC's performance. Rice husk ash (RHA) and grounded blast furnace slag (GBFS) as the cementitious material representing industrial by-product sources and recycled waste sources were used in the concrete production process [10, 13]. GBFS is a granular powder material, predominantly made from silica, alumina, and oxides; directly obtained from the iron ore and limestone used in furnaces [14]. GBFS was used to improve the overall workability of concrete pastes and increase their durability and it was also extensively utilised in UHPC [15]. GBFS can be used as a partial or full cement replacement, partial or full sand replacement, or as an additional admixture to improve the followability and performance of concrete. One of the early comprehensive study on the use of GBFS in UHPC mixes as an OPC substitute material was reported by Yazıcı, et al. [16]. It was found that the compressive and flexural strengths of UHPC were improved with only a certain percentage of GBFS in replacement of OPC. When the GBFS content was greater than 40%, the compressive strength of UHPC decreased. The finding from Yazıcı, et al. [16] was in contrast with the study by Kim, et al.

[17], in which the replacement of GBFS did not produce remarkable improvements in the compressive strength, even decreased the compressive strength of UHPC [17].

Besides GBFS, RHA is also an alternative cementitious material that is created through burning of recycled direct waste of the rice production; specifically, husks of rice grains which are discarded in the process of production [18]. According to Kang, et al. [19], approximately 150 million metric tonnes of husks are produced per year and it accounts for 21.5% on average per total weight of a rice paddy. However, RHA that is suitable for usage as an alternative cementitious material makes up only one-fifth of the total husk produced by the rice paddies [20]. Proper combustion at no more than 700°C is required for producing the husks and the produced material is powder-like ash which generally contains over 90% amorphous silica, providing excellent pozzolanic reactivity with cementitious constituents in concrete [18, 19, 21]. The use of RHA not only increases the compressive strength of concrete but also enhances the concrete's water absorbability by filling pores and voids in concrete matrices [18, 19, 21]. However, RHA was found to negatively impact the paste workability if the percentage replacement is higher than 20%, along with the increased brittleness of concrete mixes [18, 19, 21]. Giaccio, et al. [22] replaced 10% OPC with RHA in four concrete mixes with different *w/b* ratios. It was found that the mixture with the RHA exhibited higher compressive strengths compared to the control mix without RHA [22]. In a different study, He, et al. [23] investigated the effect of replacement percentages of OPC with RHA and found that the compressive strength slightly increased with the replacement percentages of OPC with the maximum increment of 15%. Meanwhile, Van Tuan, et al. [24] evaluated the possibility of using RHA to replace SF in UHPC mixtures. In their study, 40% OPC was replaced by the combination of SF and RHA. They indicated that the mixture with a ternary blend of 80% OPC, 10% RHA and 10% SF, showed a higher compressive strength than the control sample with only OPC. Van, et al. [25] also investigated the effects of RHA on the compressive strength, portlandite content, autogenous shrinkage and internal relative humidity of UHPC with/without GBFS under different treatment methods. They revealed that the incorporation of RHA and GBFS improved workability, compressive strength and autogenous shrinkage of UHPC.

From the aforementioned studies, it is clear that the replacement of the OPC with RHA and GBFS affected the compressive strength of the UHPC under quasi-static condition. However, the influence of the mentioned alternative cementitious constituents on the dynamic compressive strength of the UHPC has not been reported yet. Therefore, this study aims to investigate the quasi-static and particularly dynamic compressive properties of the UHPC with the incorporation of RHA and GBFS. To evaluate the influence of RHA and GBFS on the compressive strength of the UHPC, 30% GBFS or a combination of 15% GBFS and 15% RHA were used to replace 30% OPC (by volume) in the UHPC mixture. The dynamic compressive properties at different strain rates were investigated using a Split-Hopkinson Pressure Bar (SHPB). The dynamic compressive strength, energy absorption, and DIF were then analysed and discussed.

2. Materials and Methods

2.1 UHPC Mix Design

In this study, the effect of using alternative cementitious constituents RHA and GBFS for the OPC in UHPC was investigated. Therefore, only the amount of OPC was changed and other components in the UHPC mix, such as SP, SF, silica sand, and water, were kept constant. According to the previous study [15], the percentage of OPC replacement with RHA and GBFS was recommended in the range of 15% to 50%. Therefore, two UHPC mixes including 30% GBFS (UHPC-AC1) and 15% GBFS and 15% RHA (UHPC-AC2) were considered. To evaluate the performance of these mixes, the original UHPC mix with 80% of OPC and 20% of SF (UHPC-R1) was used as the reference mix (see Table 1).

Cementitious materials used in this study were OPC and SF from SIMCOA Operations Pty Ltd [26]. For alternative cementitious constituents, white powder slag GBFS from BGC Cement [27] and black RHA in the form of Microsilica [28] were chosen. In addition, superplasticiser (SP) from Sika [29] was used for the mixes. The chemical compositions of the cementitious materials are given in Table 2. To increase the strength of UHPC, steel fibres [30] with 13 mm in length and 2% by volume fraction were adopted for three mixes. The chemical, physical and mechanical properties of steel fibres are given in Table 3 [31]. Finally, silica sand with the maximum particle size of 0.3 mm [32] was used for the mixes.

Table 1. Summary of UHPC mixes

	Material	OPC	GBFS	RHA	SF	Silica sand	SP	Water	Steel fiber
UHPC-R1	Amount (kg/m^3)	1,000	-	-	250	1,100	70	170	156
	Binder (%)	80	-	-	20	-	-	-	-
UHPC-AC1	Amount (kg/m^3)	625	375	-	250	1,100	70	170	156
	Binder (%)	50	30	-	20	-	-	-	-
UHPC-AC2	Amount (kg/m^3)	625	187.5	187.5	250	1,100	70	170	156
	Binder (%)	50	15	15	20	-	-	-	-

Table 2. Chemical compositions of cementitious materials, (wt.%) [33, 34]

Material	SiO_2	Fe_2O_3	Al_2O_3	CaO	Na_2O	K_2O	MgO	Ti_2O_5	P_2O_5	SO_3	LOI[a]
RHA	86.20	0.43	0.46	1.10	-	4.60	0.77	-	2.43	-	4.60
GBFS	32.50	0.90	13.60	41.20	0.30	0.35	5.10	0.50	0.03	3.20	1.10

[a]LOI: Loss on ignition

Fig. 1 Steel fibre

Table 3. Properties of steel fibre [**31**]

Steel Fibre	
Chemical Properties	
Diisobutyl phthalate	< 0.28%
Steel	Remainder
Physical Properties	
Density	7,800 kg/m^3
Diameter	0.22 mm
Length	13 mm
Aspect ratio (*L/D*)	59
Shape	Straight fibre
Mechanical Properties	
Tensile strength	> 2,300 MPa
Elastic modulus	200 GPa

2.2 Sample Preparation

UHPC was mixed in a Hobart mixer (10L) at 140 rounds per minute. The procedure for preparing the UHPC mixes was similar to the previous study [25]. Firstly, silica sand, cement and silica sand were added to the mixer and mixed for 1 minute. Next, 85% water and 50% of SP were added while mixing simultaneously for 3 minutes. The remaining water was then mixed with SP before being added to the mix. Lastly, steel fibres were added in small quantities and mixed in intervals while observing for any bundling of fibres and ensuring even distribution. To ensure uniform spread of fibres within each sample, the input of fibres into the mix will be done intermittently during the mixing process. The UHPC mixes were then used for casting in 100 mm × 200 mm (diameter × length) cylindrical moulds. All cylindrical samples were compacted using a vibration table to eliminate the air trapped in the samples. The specimens were then cured in the moulds for 24 hours before they were demoulded and placed in a steam room. The steam-curing was conducted at 70°C for 72 hours and the specimens were removed and left to cool at room temperature.

Before the quasi-static testing, the samples were ground on each end using a concrete grinder to ensure the required smoothness of the tested specimens. For dynamic compression tests, the specimens had a diameter equal to that of the bar in the SHPB and an aspect ratio (*L/D*) of 0.5 to achieve the stress equilibrium condition under impact tests. According to Hao's study [35], the SHPB specimen with the aspect ratio of 0.5 could eliminate the lateral and axial inertia effects in high-speed impact tests, thus, the stress equilibrium condition can be achieved. The test specimens for dynamic tests had the size of Ø100 mm × 50 mm which were cut from Ø100 mm × 200 mm cylindrical samples using a brick saw. In total, 9 specimens for the static tests and 27 specimens for the dynamic tests were prepared.

2.3 Experimental Procedure

2.3.1 Quasi-static Test

MCC-8 compression testing machine (CONTROLS S.p.A, Liscate, Italy) was used to examine the quasi-static compressive strength of UHPC following AS1012.9 [36]. Identical cylindrical samples with the size of 100 mm × 200 mm and 100 mm × 50 mm were tested to determine the average quasi-static and dynamic compressive strength of each UHPC mix, respectively.

2.3.2 Dynamic Testing Using Split Hopkinson Pressure Bar

The dynamic compressive strength was examined using the SHPB, as shown in Fig. 2. To investigate the strain rate effects, different levels of impact loading was applied to the specimens, which correspond to the chamber pressures of 300 kPa, 400 kPa and 450 kPa. Petroleum jelly was used on both tested surfaces of each sample to minimize friction at the interfaces. According to Pham, et al. [37], the abundance of the friction forces at the specimen ends may result in overestimating the dynamic strength of tested samples.

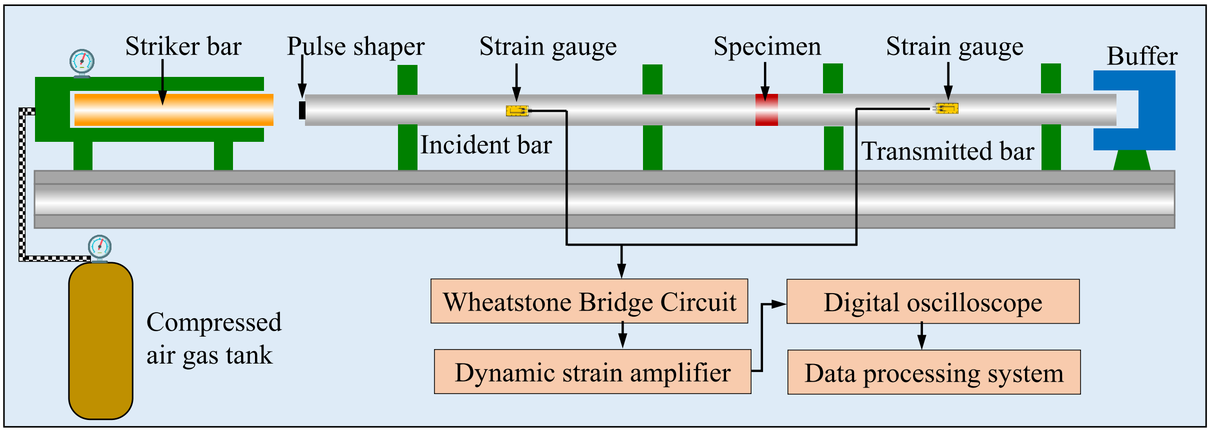

Fig. 2. Schematic diagram of an SHPB system with a pulse-shaper

The Ø100 mm SHPB system consists of a 5,500 mm incident bar and a 3,000 mm transmitted bar. Strain gauges were installed on incident bar and transmitted bar to monitor strain of each bar. The bars are made of stainless steel with a density of 7,800 kg/m^3 and Young's modulus of 210 GPa. A high-speed camera with a sampling rate of 40,000 frames per second was used to capture the progressive failure of the tested specimens.

According to one-dimensional stress wave propagation, the stress (σ), strain rate ($\dot{\varepsilon}$), and strain (ε) of the specimen can be determined from the following equations [38]:

$$\sigma(t) = E\left(\frac{A}{A_s}\right)\varepsilon_T(t) \qquad (1)$$

$$\dot{\varepsilon}(t) = -\frac{2C_0}{L}\varepsilon_R \quad (2)$$

$$\varepsilon(t) = \int_0^T \dot{\varepsilon}(t)dt \quad (3)$$

where A, E, and C_0 are the cross-sectional area, Young's modulus, and elastic wave velocity of the bars; A_s and L are the cross-sectional area and length of the tested specimen, and ε_T and ε_R are the measured transmitted and reflected strain, respectively.

For the data derived from these equations to be valid, the stress equilibrium in the longitudinal direction of the specimen must be achieved. For brittle materials, such as concrete, specimen failure may occur before axial stress equilibrium. This is due to failure strain being relatively small in brittle materials and the rise-time of the incident pulse being short in a conventional SHPB test [39]. To extend the rise time so that the axial stress equilibrium can be achieved in a specimen, a pulse-shaper may be attached to the free end of the incident bar to increase the rise time of the incident pulse. Therefore, the rubber pulse-shaper suggested in previous studies [40] was adopted in this study (see Fig. 3b).

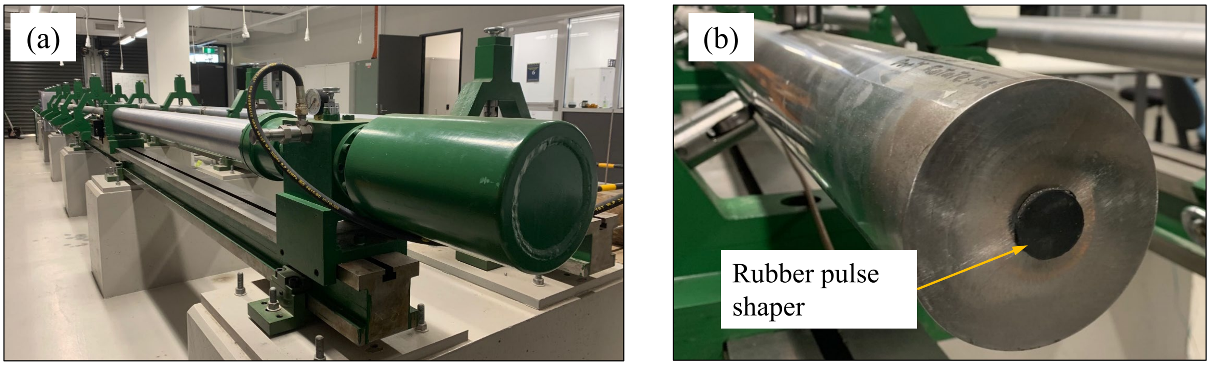

Fig. 3. (a) SHPB system and (b) rubber pulse-shaper

3. Experimental Results

3.1 Quasi-static Compressive Testing Results

Fig. 4 shows the static compressive strength of the three mixes. It is obvious that the UHPC-R1 mix achieved the highest average static compressive strength of 159.3 MPa. Meanwhile, the two alternative cementitious mixes (UHPC-AC1 and UHPC-AC2) performed favourably in comparison to the reference mix UHPC-R1. Particularly, Mix UHPC-AC1 with 30% GBFS achieved an average static compressive strength of 151.3 MPa while Mix UHPC-AC2 with 15% GBFS and 15% RHA achieved an average strength of 143.5 MPa. As a result, the compressive strength of UHPC decreased by about 5% and 10% when replacing OPC with 30% GBFS and 15% GBFS + 15% RHA in UHPC. It can be seen that the compressive strength of the UHPC incorporating GBFS and RHA was comparable with that of the reference mix. Therefore, the use of alternative cementitious constituents GBFS and RHA to partially replace OPC is a promising solution to produce environmentally friendly UHPC, minimizing the impact of CO_2 emission into the environment.

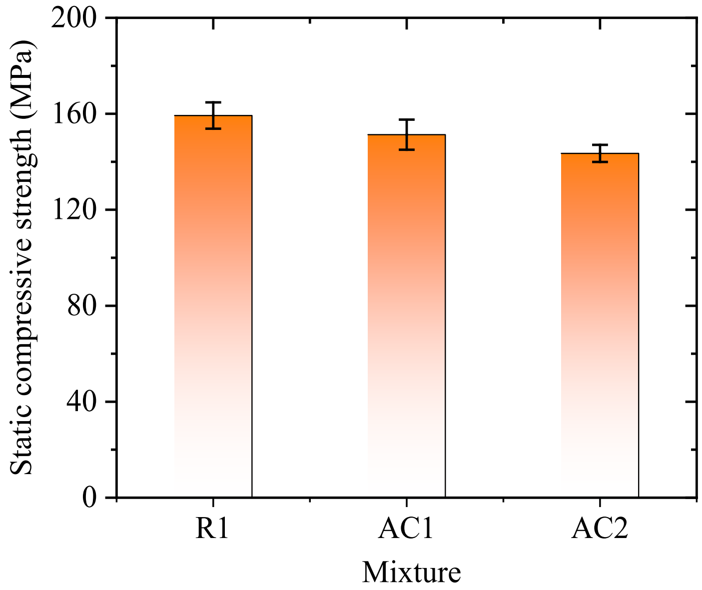

Fig. 4. Quasi-static compressive strength of UHPC of the three mixes

Fig. 5 shows the fracture pattern of the UHPC specimens of the three mixes after the quasi-static compression testing. It can be seen that all the specimens displayed similar modes of failure. Particularly, many small cracks occurred at the specimen end, following by a major crack breaking down in the specimens (UHPC-AC2). Meanwhile, the cracks propagated from the top to the middle of the specimen (UHPC-R1) or one-third of the specimen (UHPC-AC1) in an inclined direction.

UHPC-R1 UHPC-AC1 UHPC-AC2

Fig. 5. Quasi-static failure modes of three UHPC specimens

3.2 Dynamic Compressive Testing Results

3.2.1 Stress Equilibrium

Dynamic compressive testing at various strain rates was carried out using the SHPB. The crucial importance of SHPB testing and analysis is ensuring that the dynamic stress equilibrium is achieved for the tested samples. Therefore, the stress equilibrium was checked for all the tested specimens by assessing the matching of the transmitted stress and the sum of the incident and reflected stresses. Fig. 6 shows an example of a stress equilibrium check for a tested sample. It is clear that the Incident + Reflected waves are comparable with the transmitted wave for the first phase, reaching the same level of the first peak as the Transmitted wave.

After the peak stress, the mismatch in transmitted and incident + reflected waves was observed in the later stage in UHPC. This phenomenon often occurs when investigating the dynamic behaviour of UHPC, but it is hardly found in normal concrete. This can be explained that the post-peak behaviour of UHPC is ductile, where the compressive stress slightly reduces after the peak. Therefore, it is difficult to achieve the stress equilibrium at a later stage since the dynamic stress wave equilibrium is usually achieved in a short period. Meanwhile, the normal strength concrete without fibres is brittle and then the compressive stress reduces significantly after peaks.

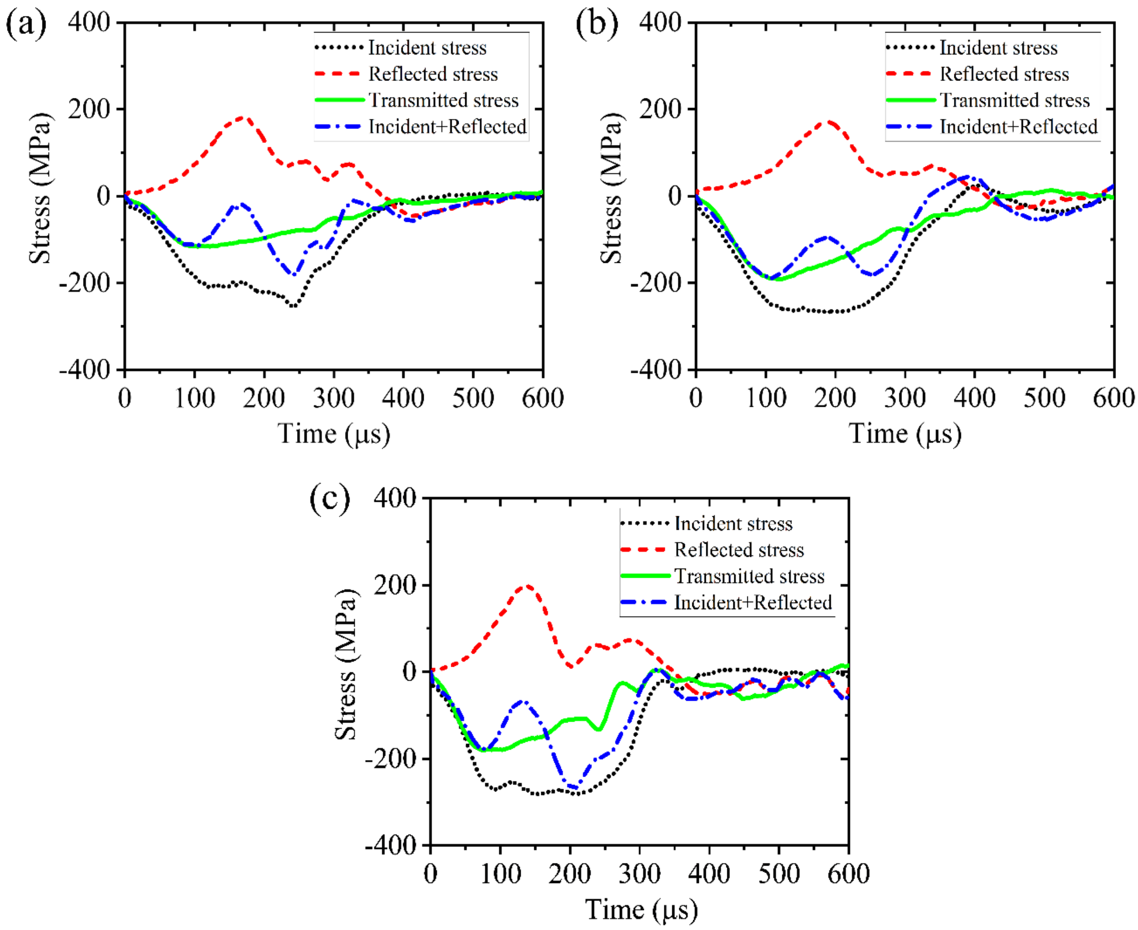

Fig. 6. Stress histories of the tested specimens: (a) UHPC-R1, (b) UHPC-AC1 and (c) UHPC-AC2

It is noted that, in this study, rubber pulse shapers were also used to increase the rise time and achieve the stress equilibrium based on the suggestion of the previous study on the dynamic compressive strength of UHPC [41] and rubberised concrete [37]. According to Hassan and Wille [41], the pulse shaper thickness affected the rise time of the incident wave, while the diameter of the pulse shaper affected the slope of the ascent and the descent of the incident wave form. Although with the same material (rubber) and shape of the pulse shapers, the rise time of UHPC in this study was different from rubberised concrete reported in the previous study [37]. This indicated that the rise time was also affected by the strength of the test specimen as well as other factors such as intensity of the impact and surface-to-surface contact between the bars and specimen. The surface-to-surface contact between the specimen and the incident bar affected the rise time that was reported by Guo, et al. [42]. Ideally, both ends of the tested specimens should also be perfectly parallel and flat to achieve full surface contact with the bars in the SHPB system. In addition, steel fibres tended to stick out of the surfaces of the specimens caused the surface roughness, even after grinding. As a consequence, the distribution of stress during loading was not completely uniform, thus, it was difficult to achieve a perfect stress equilibrium condition for the UHPC. Considering those difficulties, only specimens achieving the stress equilibrium condition were reported and the presented data in this study show the reasonable stress equilibrium condition.

3.2.2 Strain rate determination

The strain rate of the three UHPC mixtures was time-dependent and there are various methods for strain rate determination. The strain rate was determined by taking the mean strain rate over the loading period [43] or considering the strain rate at peak stress [37]. In this study, the strain rate was determined for each sample using the strain rate at the peak stress as also adopted in the previous studies [37], see Fig. 7.

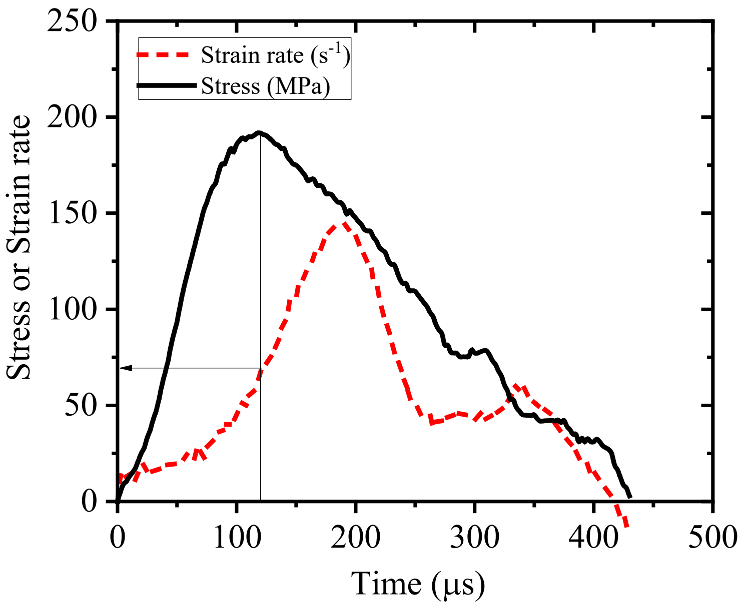

Fig. 7. Strain rate determination

3.3 Failure Processes and Failure Modes

Fig. 8 shows the final failure modes of the tested specimens, in which Figs. 8a, 8b, and 8c illustrate the failure mode of UHPC-R1, UHPC-AC1 and UHPC-AC2, respectively. It was observed that the failure mode of Mix UHPC-R1 shows a major crack across the sample section and many spalling failures were also observed around the perimeter. Meanwhile, the failure mode of UHPC-AC1 consisted of several small cracks on the cross-section of the sample. Similar to Mix UHPC-R1, many spalling failures were observed around the perimeter of the specimens of Mix UHPC-AC1. The failure mode of UHPC-AC2 contained severe spalling damage compared to Mixes UHPC-R1 and UHPC-AC1. In general, the failure modes of these mixes were similar.

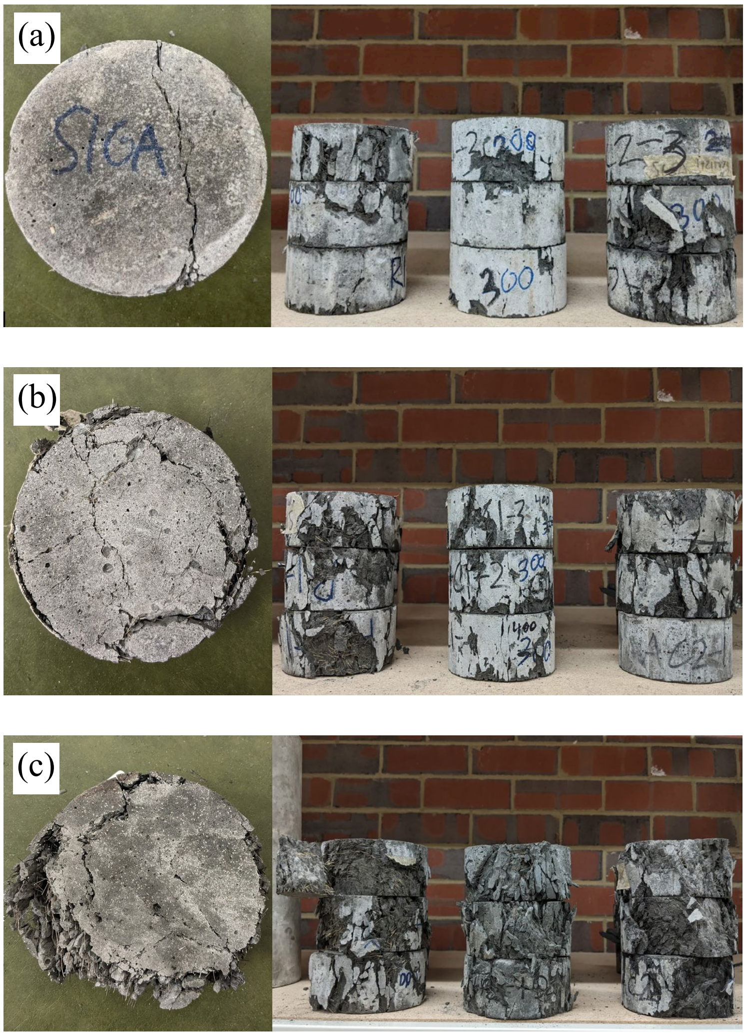

Fig. 8. Failure modes of a) UHPC-R1, (b) UHPC-AC1 and (c) UHPC-AC2

Fig. 9 shows the progressive failure of the tested specimens using a high-speed camera at a rate of 40,000 frames per second. It can be seen that the cracks initiated from both sides of the specimens and developed into the mid-region, demonstrating the stress equilibrium condition. The number of cracks was not significantly different between the three mixes. When the specimen was further loaded, initial cracks developed. The bridging effect of steel fibres prominently slowed down the crack development and crack propagation.

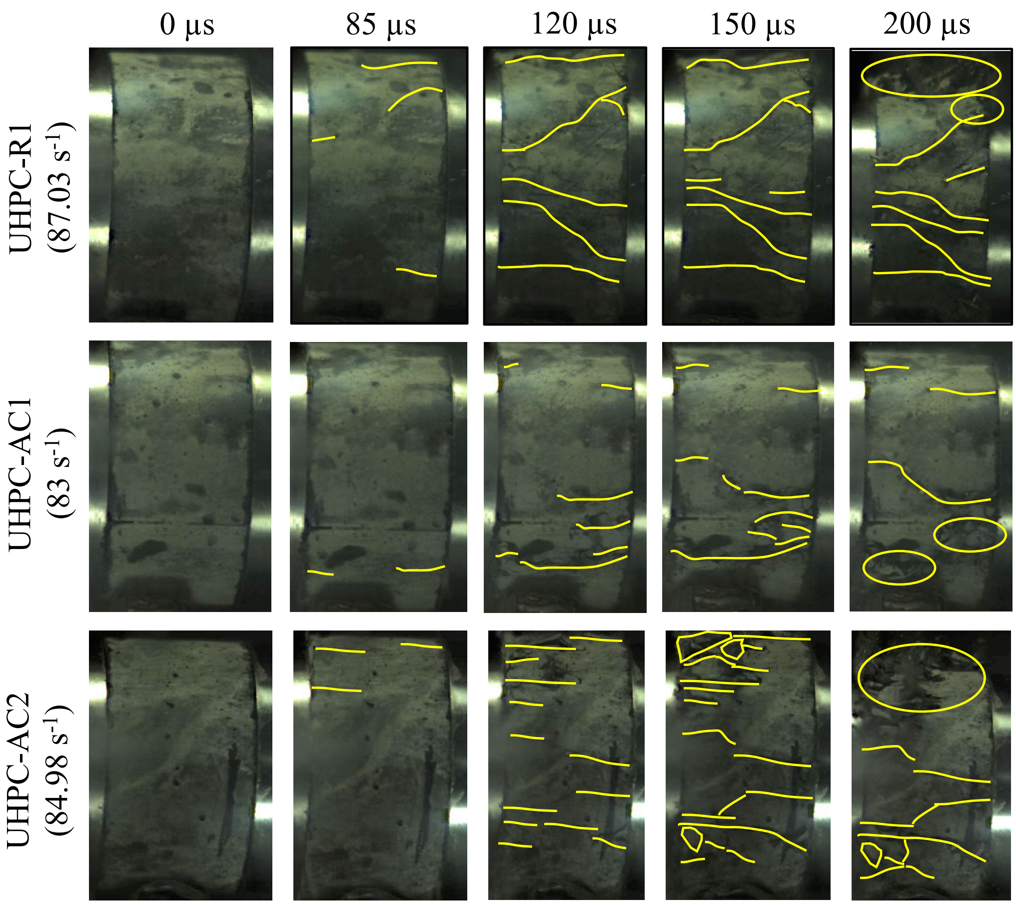

Fig. 9. Progressive failure pattern of three UHPC mixes (oval shape shows the spalling).

3.4 Stress-Strain Curves and Energy Absorption

The stress-strain curves of UHPC and the corresponding strain rates were obtained from the test data and are shown in Fig. 10. Generally, the initial stage of the stress-strain curves followed a linear trend, indicating elastic deformation, before gradually curving towards the peak stress. The compressive stress then began a post-peak descending branch due to its ductile behaviour as reported in the previous studies due to the bridging effect of steel fibres. When incorporating the alternative cementitious constituents GBFS and RHA, the stress-strain curves of the alternative mixes UHPC-AC1 and UHPC-AC2 were similar to that of Mix UHPC-R1 with OPC cement, as shown in Figs. 10a, 10b and 10c.

Fig. 10d illustrates the dynamic compressive strengths of UHPC with three different mixes R1, AC1 and AC2. It can be seen that the dynamic compressive strength of UHPC with the three different mixes R1, AC1 and AC2 was not significantly different when the strain rate increased. This means that the proposed mixes of UHPC in this study exhibit marginal strain rate sensitivity. Fig. 10d also indicates that the dynamic compressive strength of the three mixes was similar within the range of studied strain rates. In another word, the OPC in the UHPC mix can be alternated with the recycled cementitious constituents such as GBFS and RHA without scarifying the dynamic compressive strength.

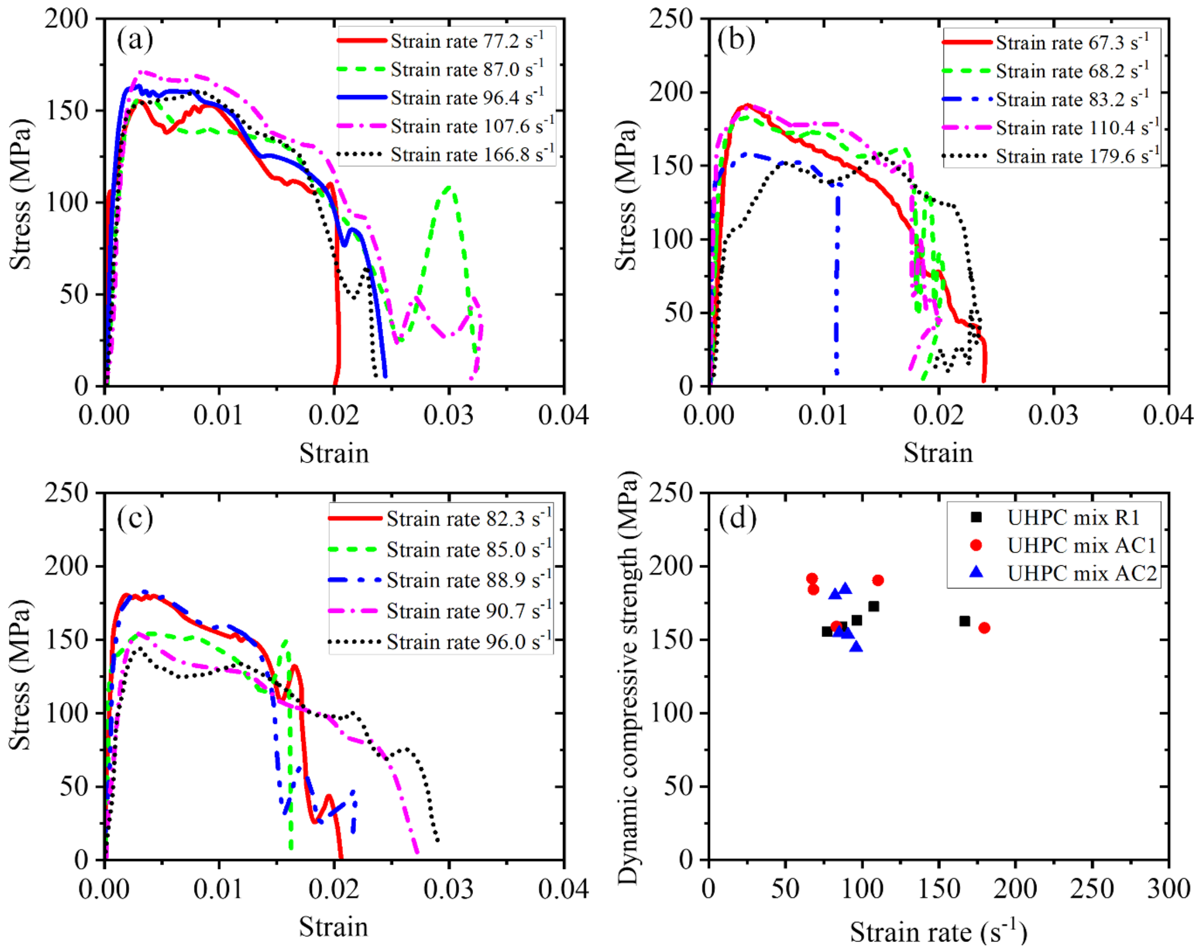

Fig. 10. Stress-strain curves of (a) UHPC-R1, (b) UHPC-AC1 and (c) UHPC-AC2; and (d) dynamic compressive strength

Fig. 11 illustrates the energy absorption of three different mixes at various strain rates. In this figure, the energy absorption was determined from the enclosed area under the stress-strain curves in Figs 10a-10c. For each mix, the energy absorption slightly increases with strain rate, which has also been reported in the previous studies [44]. Meanwhile, the present results also display a considerable variation. These variations due to the fluctuation of the stress-strain curves which caused by the different response of the specimens under different strain rates. In addition, results from SHPB tests usually fluctuate due to the complexity of the tests and the nature of the dynamic testing as observed in previous studies [45].

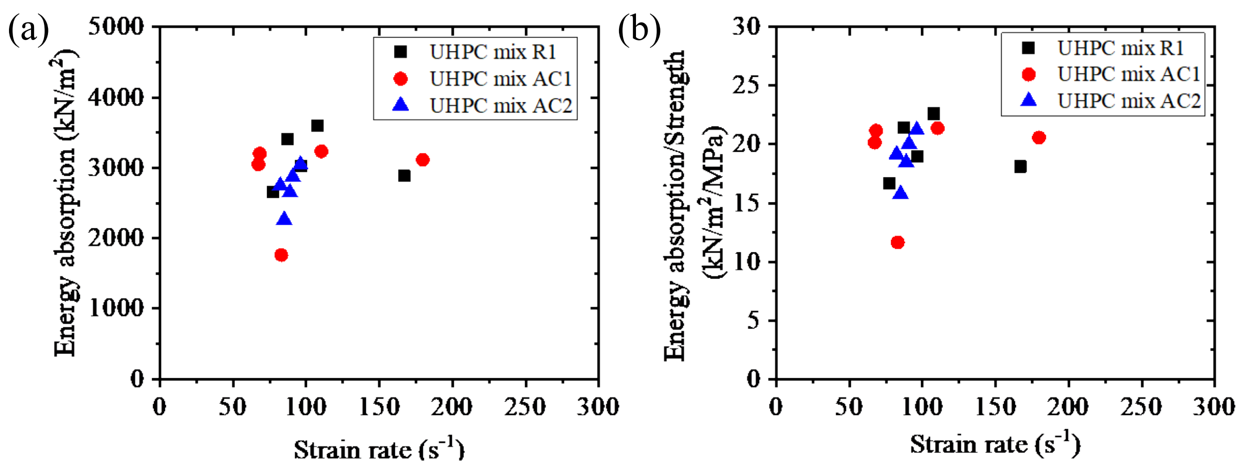

Fig. 11. (a) Energy absorption and (b) normalised energy absorption of three UHPC mixtures

Table 4. Dynamic Testing Results

UHPC Mix	Sample ID	Strain Rate (1/s)	Static Compressive Strength (MPa)	Dynamic Compressive Strength (MPa)	Dynamic Increase Factor (DIF)	Energy Absorption (kN/m^2)
	R1-300-1	77		155.4	0.98	2654
	R1-450-1	87		158.8	1.00	3409
R1	R1-450-2	96	159.3	163.2	1.02	3021
	R1-450-3	108		172.5	1.08	3601
	R1-400-1	167		162.6	1.02	2884
	AC1-400-1	67		191.7	1.27	3048
	AC1-400-2	68		184.2	1.22	3202
AC1	AC1-300-1	83	151.3	159.0	1.05	1762
	AC1-400-3	110		190.4	1.26	3232
	AC1-300-2	180		158.0	1.04	3113
	AC2-400-1	82		180.2	1.26	2746
	AC2-300-1	85		154.7	1.08	2261
AC2	AC2-400-2	89	143.5	184.2	1.28	2648
	AC2-450-1	91		153.6	1.07	2871
	AC2-450-2	96		144.6	1.01	3042

4. Discussions

4.1 Quasi-Static Performance of UHPC

As stated in the previous section, the quasi-static compressive strength for all the UHPC mixes was in the range of 143.5-159.3 MPa, which is far higher than 120 MPa for classifying the UHPC category under ASTM C1856 [46]. However, according to the ACI standard [47], the compressive strength of UHPC should be greater than 150 MPa, leading to only two mixtures including UHPC-R1 and UHPC-AC1 satisfy this criteria. The compressive strength of Mix UHPC-AC2 was 143.5 MPa that is 4.5% less than the required minimum compressive strength of UHPC according to ACI standard [47]. Therefore, with the incorporation of the alternative cementitious constituents GBFS and RHA, the alternative mix did not meet the minimum requirement of UHPC according to ACI standard.

As mentioned above, when incorporating the alternative cementitious constituents, the compressive strength of the UHPC mixes slightly decreased. This observation can be explained that GBFS slowed down the hydration process and setting time, which caused low early strength. According to Lee and Lee [48], the development of the compressive strength of GBFS based concrete depended on the GBFS replacement ratio and concrete curing age. The GBFS glassy compounds reacted slowly with water, and it took time to obtain hydroxyl ions to break the glassy slag parcels from the hydration products of OPC at an early age [49]. These findings were also consistent with previous studies [15, 49]. Most of the studies reported that the compressive strength of the UHPC mix at an early age decreased with the percentage of the GBFS replacement. The compressive strengths at 3 days of the UHPCs with slag decreased by around 4.8–18.1% regarding the reference specimens [49]. Meanwhile, Pyo and Kim [15] revealed that the incorporation of GBFS caused a decrease of the compressive strength at 1 day and 3 days by 39% and 18%, respectively. It can be seen that GBFS tended to decrease the early compressive strength of UHPC due to its low hydration activity as well as retarding effect on the cement hydration.

The compressive strength of UHPC with GBFS can be improved by increasing the curing process. When the curing time is long enough, normally more than 28 days, the secondary pozzolanic reaction between GBFS and $Ca(OH)_2$ in the pore solution produces additional C-S-H gel (Calcium Silicate Hydrate), which increases the packing density of UHPC, leading to the increased compressive strength of UHPC [45]. Besides, Liu et al. [13] found that the compressive strength increased up to 9% when the GBFS content increased to 40% of the binder due to the secondary pozzolanic reaction of GBFS. Meanwhile, Shi, et al. [50] indicated that the compressive strength of UHPC with GBFS can be improved by using the autoclave curing with a temperature of 180^{o}C for 8h as compared to the steam curing with a temperature of 80^{o}C for 48h.

For Mix UHPC-AC2 with GBFS and RHA, the RHA absorb water. Meanwhile, GBFS required a higher amount of water to attain proper hydration for achieving higher compressive strength as discussed above [15-17]. As a result, Mix UHPC-AC2 which incorporated both GBFS and RHA required more water and superplasticiser in comparison to reference mix UHPC-R1 to maintain similar workability. However, in this study, water was constrained to be the same in three mixes. Therefore, Mix UHPC-AC2 with GBFS and RHA had less water for GBFS to attain proper hydration compared to the mix UHPC-AC1, leading to the compressive strength of the mix UHPC-AC2 slightly lower than that of the mix UHPC-AC1.

4.2 Dynamic Performance of UHPC

To investigate the dynamic performance of three UHPC mixes, the dynamic increase factors (DIF) defined by the ratio between dynamic compressive strength and static compressive strength for all the specimens are calculated and shown in Fig. 12. It is obvious that all the specimens displayed less strength enhancement at high strain rate as compared to normal concrete (see black line in Fig. 12). In fact, when the strain rate increased, the DIF did not change significantly, especially those of the mix UHPC-R1. This findings also agreed well with previous studies [44, 51] where UHPC showed marginal sensitivity to strain rate as shown in Fig. 12.

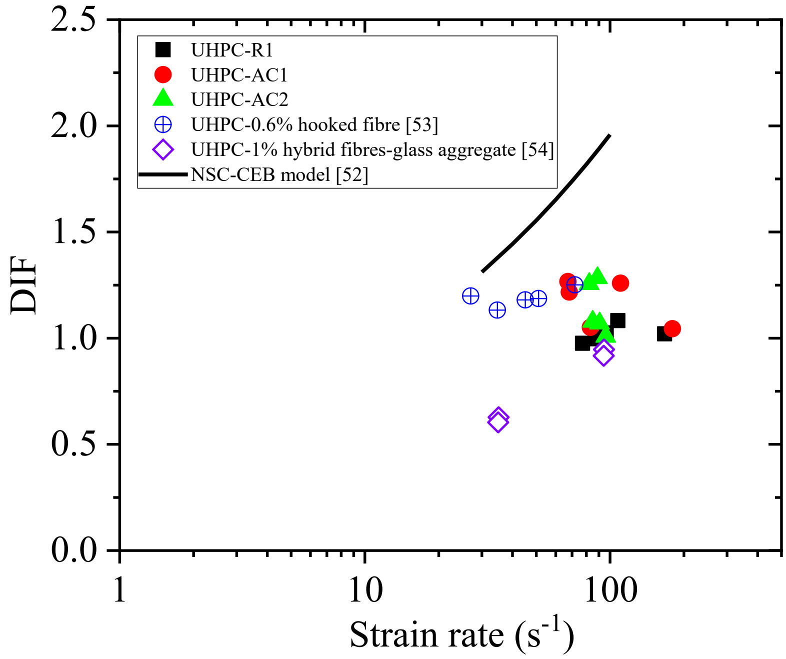

Fig. 12. Comparison of DIF with different UHPC mixes

To further investigate the sensitivity of UHPC to strain rate, the relationship between the DIF and strain rate of the previous studies and CEB model [52] is compared and shown in Fig. 12. As shown, the DIF of Mix UHPC-R1 is almost constant when increasing strain rate from 77.2 s^{-1} to 107.6 s^{-1}, demonstrating marginal strain rate sensitivity. Meanwhile, the DIF of UHPC-AC1 and UHPC-AC2 do not show an obvious increase with the strain rate but oscillate slightly in the strain rate range achieved in the tests in this study. These oscillations can be attributed to the testing errors. It can be seen that the DIF of Mixes UHPC-AC1 and UHPC-AC2 were in the range from 1.044 to 1.267 and 1.008 to 1.284, which were slightly higher than that of the UHPC-R1, respectively. These results indicate that the compressive strength of UHPC-AC1 and UHPC-AC2 are not as sensitive as normal concrete to strain rate in the narrow strain rate range obtained in this study. Further tests are needed to investigate the strain rate effects on the compressive strength of UHPC-AC1 and UHPC-AC2 in a wide range of strain rates.

The DIF of the UHPC mixes in this study was also compared to that of another UHPC in the previous studies [53, 54] and normal strength concrete(NSC) [52]. According to Malvar and Crawford [52], the DIFs for NSC (f_{cs} = 52.5 MPa) can be obtained from empirical formulae as below:

$$DIF = \frac{f_c}{f_{cs}} = \begin{cases} \left(\dfrac{\dot{\varepsilon}}{\dot{\varepsilon}_s}\right)^{1.026\alpha} & \text{for } \dot{\varepsilon} \le 30\text{s}^{-1} \\ \gamma_s \left(\dfrac{\dot{\varepsilon}}{\dot{\varepsilon}_s}\right)^{1/3} & \text{for } \dot{\varepsilon} > 30\text{s}^{-1} \end{cases} \quad (4)$$

where f_c is the dynamic compressive strength at $\dot{\varepsilon}$, f_{cs} is the static compressive strength at $\dot{\varepsilon}_s$, $\dot{\varepsilon}$ is the strain rate in the range of 30×10^{-6} to 300 s^{-1}, $\dot{\varepsilon}_s$ is the static strain rate 30×10^{-6}, $\log\gamma_s = 6.156\alpha - 2$, $\alpha = 1/(5 + 9f_{cs}/f_{co})$ and f_{co} = 10 MPa.

It is clear that the DIFs of the three UHPC mixes in this study were similar to those of the typical UHPC [53] and slightly higher than those of eco-friendly UHPC with recycled glass aggregate [54], demonstrating the potential use of recycled cementitious materials such as GFBS and RHA for the development of new UHPC subjected to impact loading. However, when comparing to NSC [52], the DIFs of the proposed UHPC were much lower than those of NSC [52]. This observation confirms that UHPC is less sensitive to strain rate than NSC, which can be attributed to several reasons: (1) existence of coarse aggregates in NSC, (2) viscosity caused by air and water trapped in voids of the matrix and (3) effect of crack velocity in concrete material with strain rate. Firstly, under quasi-static loading, cracks initiate and propagate through weak interfacial transition zones between coarse aggregates and the matrix. Under a high loading rate, NSC underwent damage cutting through coarse aggregates which were much stronger than the matrix, leading to higher dynamic compressive strength and DIF. UHPC usually does not contain coarse aggregates, thus, this effect can be eliminated for UHPC under a high loading rate. Secondly, the porosity with entrapped air and water also affects the dynamic properties of concrete. UHPC has a very low void content as compared to that of NSC. Therefore, the influence of viscosity on the dynamic properties of UHPC is thus also nominal. Finally, it is known that the crack velocity in concrete material increased with strain rate. Under similar strain rate loading, UHPC had a slower crack expansion due to the fibre-bridging effect compared to NSC, resulting in a lower strength enhancement. These phenomena explain why UHPC is less sensitive to strain rate as compared to NSC, which was experimentally confirmed by the results of this study and previous studies [53, 55].

Fig. 11 illustrates the energy absorption of the three mixes of UHPC at various strain rates. In this figure, the energy absorption of the UHPC was determined from the enclosed area under the stress-strain curves in Figs. 10a-10c. For each mix, the energy absorption slightly increases with strain rate, which has also been reported in the previous studies [44]. It is also evident from Fig. 11 that Mixes UHPC-AC1 and UHPC-AC2 exhibited comparable energy absorption capacities to Mix UHPC-R1 at same strain rates. This is because three mixes displayed a similar dynamic compressive strength, residual strain and stress-strain relation characteristics as shown in Fig. 10. Regarding the energy absorption capacity of Mixes UHPC-AC1 and UHPC-AC2, it can be concluded that the alternative cementitious constituents such as GBFS and RHA can be used for manufacturing the UHPC for dynamic loading conditions.

4.3 Environmental Evaluation

As mentioned previously, the aims of using GBFS and RHA are mainly to reduce environmental impact and reduce the material costs. This study only focused on the environmental impact because comparing the material costs were impractical owing to the varying costs among different countries/providers. Nowadays, the most critical environmental impact is carbon dioxide (CO_2) emission. Therefore, to evaluate the environmental friendly performance of the alternative mixes UHPC-AC1 and UHPC-AC2, their embedded CO_2 emission (e-CO_2) were estimated and compared to that of the reference UHPC-R1. Table 5 provides the e-CO_2 data of the raw materials used in the UHPC mixes. The e-CO_2 of the three mixes of UHPC in this study was calculated as the sum of the values obtained by multiplying the carbon footprint values (Table 5) with the volume percentage of materials in each UHPC mixture. In addition, in this study, the UHPC mixes were cured using a steam room at 70°C for 72 h. Therefore, the CO_2 emission during the curing process was also taken into account. The CO_2 emission of steam curing was about 2.49 kg/m^3/h CO_2 based on the investigation in the previous study [56]. As mentioned previously, the constant temperature time was 72 h and the time for gradual heating was approximately 2.5 h [50], leading to a total of 74.5 h for estimations. Consequently, the CO_2 emission of steam curing was calculated to be 74.5 h × 2.49 kg/m^3/h = 185.5 kg/m^3. The total CO_2 emission for each UHPC mix is shown in Table 6.

The optimal UHPC mix should have high strength and low environmental impact. Therefore, e-CO_2 index (*CI*) defined by the ratio between e-CO_2 and the static compressive strength (σ) were introduced in Eq. 5.

$$CI = \frac{e - CO_2(\text{kg/m}^3)}{\sigma(\text{MPa})} \tag{5}$$

Table 5. The e- CO_2 of the raw materials

Items	e-CO_2	Reference
Cement	0.8300	[50]
RHA	0.1032	[57]
GBFS	0.0190	[50]
SF	0.0140	[58]
Quartz sand	0.0100	[50]
SP	0.7200	[50]
Water	0.0003	[50]
Steel fiber	1.4965	[50]

Table 6. The embodied carbon dioxide and energy consumption of the raw materials

Mixture	Compositions (kg/m^3)								e-CO_2 curing process (kg/m^3)	Total e-CO_2 (kg/m^3)
	Cement	SF	GBFS	RHA	Sand	Water	SP	Steel fiber		
UHPC-R1	1000	250	-	-	1100	170	70	156	185.5	1313.9
UHPC-AC1	625	250	375	-	1100	170	70	156	185.5	1009.8
UHPC-AC2	625	250	187.5	187.5	1100	170	70	156	185.5	1025.6

Fig. 13 illustrates the comparison of the *CI* index of the three UHPC mixtures investigated in this study. It is obvious from the figure that the alternative mixes UHPC-AC1 and UHPC-AC2 have a lower *CI* index compared to the reference mix UHPC-R1. This finding demonstrates the merit of using GBFS and RHA as a binder component in making UHPC with an attempt to reduce the environmental impact. When comparing the two newly developed mixes UHPC-AC1 and UHPC-AC2, it is clear that the *CI* index of Mix UHPC-AC1 with GBFS is lower than that of Mix UHPC-AC2 with GBFS+RHA. Therefore, Mix UHPC-AC1 with GBFS is more efficient in terms of high compressive strength and low environmental impact. However, in this study, only one mixture with a volume fraction of the RHA was considered, thus, further testing would be required to investigate the compressive performance of the UHPC with different volume fractions of the GBFS and RHA to conclude the effects of these components on *CI* index.

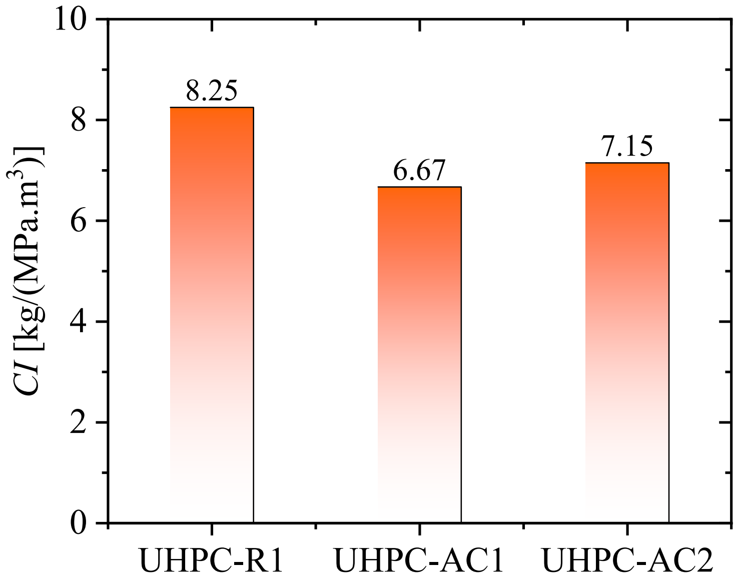

Fig. 13. Comparison of e-CO2 emissions of the three mixtures UHPC

To demonstrate the developed UHPC with the GBFS and RHA are efficient and eco-friendly materials, the e-CO_2 emissions of Mixes UHPC-AC1 and UHPC-AC2 were compared to other UHPCs in the literature, as shown in Fig. 14. Yu, et al. [49] summarized the e-CO_2 emissions of a number of studies on UHPC and found a linear relationship between e-CO2 and compressive strength as illustrated in the trendline (see Fig. 14). Therefore, UHPC with the data points on or below the trend line have a lower environmental impact than the average value. It is clear that the compressive strength of Mixes UHPC-AC1 and UHPC-AC2 developed in this study are higher than that of most of UHPC developed in the previous studies. Moreover, it is important to notice that the data points representing the UHPC-AC1 on the trendline, demonstrating the UHPC-AC1 mix is in the common region of the UHPC investigated in previous studies. So far, it can be seen that the compressive strength and e-CO_2 are dependent on the volume fractions of OPC, GBFS and RHA. Therefore, UHPC can be designed with less environmental impact and reasonable compressive strength by optimizing the binder material components and curing conditions.

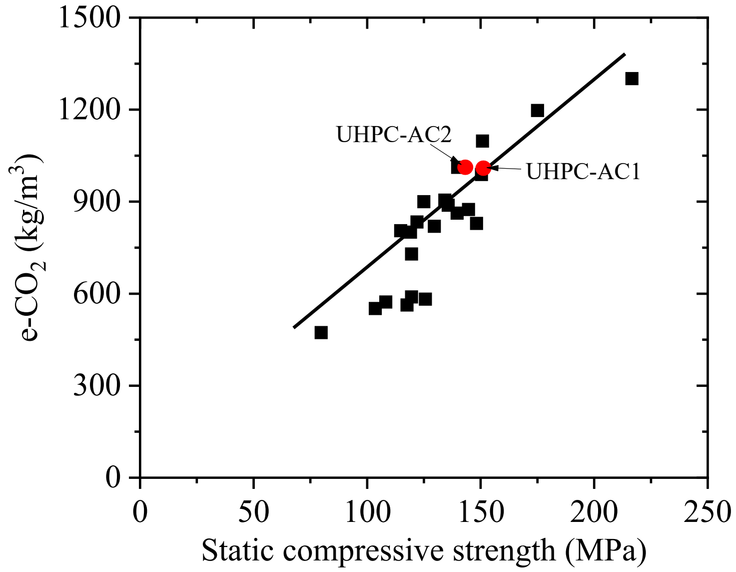

Fig. 14. Comparison of e-CO2 emission of the developed UHPC-AC1 and UHPC-AC2 in this study and other UHPC summarised in reference [49]

5. Conclusion

This study successfully investigated the effect of alternative cementitious constituents on the compressive performance of UHPC. The static and dynamic compressive properties of the newly developed UHPC were then experimentally investigated. The following findings have been drawn based on the results presented in this paper:

1. The findings have indicated that 30% replacement of OPC with GBFS or GBFS and RHA in a predetermined UHPC mixture still produced concrete with high static and dynamic compressive strength. Particularly, the static compressive strength of the mix UHPC-AC1 with 30% GBFS and the mix UHPC-AC2 with 15% GBFS and 15% RHA replacement of OPC were 151.3 MPa and 143.5 MPa, respectively.
2. The impact testing indicated that the dynamic compressive strength of the UHPC with three different mixes UHPC-R1, UHPC-AC1 and UHPC-AC2 are not as sensitive to strain rate as normal concrete.

3. The alternative mixes UHPC-AC1 and UHPC-AC2 had a lower CI index compared to the reference UHPC-R1, demonstrating the merit of using GBFS and RHA as a binder component in making the UHPC with an attempt to reduce the environmental impact while not greatly reducing the UHPC strength.

The experimental results showed that RHA and GBFS are potential cementitious constituents to partially replace OPC in UHPC to produce efficient UHPC with high strength and low environmental impact.

Acknowledgements

The financial support from the Australian Research Council Laureate Fellowships FL180100196 is acknowledged. The financial support from Small Grant, Curtin University is also acknowledged.

References

[1] Y.-W. Chan, S.-H. Chu, Effect of silica fume on steel fiber bond characteristics in reactive powder concrete, Cem. Concr. Res. 34(7) (2004) 1167-1172.

[2] C. Shi, Z. Wu, J. Xiao, D. Wang, Z. Huang, Z. Fang, A review on ultra high performance concrete: Part I. Raw materials and mixture design, Construction and Building Materials 101 (2015) 741-751.

[3] F. de Larrard, T. Sedran, Optimization of ultra-high-performance concrete by the use of a packing model, Cement and concrete research 24(6) (1994) 997-1009.

[4] P. Richard, M. Cheyrezy, Composition of reactive powder concretes, Cement and concrete research 25(7) (1995) 1501-1511.

[5] K. Wille, A.E. Naaman, G.J. Parra-Montesinos, Ultra-High Performance Concrete with Compressive Strength Exceeding 150 MPa (22 ksi): A Simpler Way, ACI materials journal 108(1) (2011).

[6] D.-Y. Yoo, N. Banthia, J.-Y. Lee, Y.-S. Yoon, Effect of fiber geometric property on rate dependent flexural behavior of ultra-high-performance cementitious composite, Cement and Concrete Composites 86 (2018) 57-71.

[7] A. Bentur, S. Mindess, N. Banthia, Behavior of reinforced concrete under impact: The effect of concrete strength, Society for Experimental Mechanics (1987) 449-458.

[8] E. Ghafari, H. Costa, E. Júlio, Critical review on eco-efficient ultra high performance concrete enhanced with nano-materials, Constr. Build. Mater. 101 (2015) 201-208.

[9] I. Talebinejad, S.A. Bassam, A. Iranmanesh, M. Shekarchizadeh, Optimizing mix proportions of normal weight reactive powder concrete with strengths of 200–350 MPa, Proceedings of the International Symposium on UHPC, Kassel, Germany, 2004, pp. 133-141.

[10] R. Yu, P. Spiesz, H. Brouwers, Development of Ultra-High Performance Fibre Reinforced Concrete (UHPFRC): Towards an efficient utilization of binders and fibres, Construction and building materials 79 (2015) 273-282.

[11] O.M. Abdulkareem, A.B. Fraj, M. Bouasker, A. Khelidj, Mixture design and early age investigations of more sustainable UHPC, Construction and Building Materials 163 (2018) 235-246.

[12] K.-H. Yang, Y.-B. Jung, M.-S. Cho, S.-H. Tae, Effect of supplementary cementitious materials on reduction of CO2 emissions from concrete, Journal of Cleaner Production 103 (2015) 774-783.

[13] Z. Liu, S. El-Tawil, W. Hansen, F. Wang, Effect of slag cement on the properties of ultra-high performance concrete, Constr. Build. Mater. 190 (2018) 830-837.

[14] R.K. Patra, B.B. Mukharjee, Influence of incorporation of granulated blast furnace slag as replacement of fine aggregate on properties of concrete, Journal of cleaner production 165 (2017) 468-476.

[15] S. Pyo, H.-K. Kim, Fresh and hardened properties of ultra-high performance concrete incorporating coal bottom ash and slag powder, Construction and Building Materials 131 (2017) 459-466.

[16] H. Yazıcı, M.Y. Yardımcı, H. Yiğiter, S. Aydın, S. Türkel, Mechanical properties of reactive powder concrete containing high volumes of ground granulated blast furnace slag, Cement and Concrete Composites 32(8) (2010) 639-648.

[17] H. Kim, T. Koh, S. Pyo, Enhancing flowability and sustainability of ultra high performance concrete incorporating high replacement levels of industrial slags, Construction and Building Materials 123 (2016) 153-160.

[18] H. Huang, X. Gao, H. Wang, H. Ye, Influence of rice husk ash on strength and permeability of ultra-high performance concrete, Construction and Building Materials 149 (2017) 621-628.

[19] S.-H. Kang, S.-G. Hong, J. Moon, The use of rice husk ash as reactive filler in ultra-high performance concrete, Cement and Concrete Research 115 (2019) 389-400.

[20] B.S. Thomas, Green concrete partially comprised of rice husk ash as a supplementary cementitious material–A comprehensive review, Renewable and Sustainable Energy Reviews 82 (2018) 3913-3923.

[21] A.P. Gursel, H. Maryman, C. Ostertag, A life-cycle approach to environmental, mechanical, and durability properties of "green" concrete mixes with rice husk ash, Journal of Cleaner Production 112 (2016) 823-836.

[22] G. Giaccio, G.R. de Sensale, R. Zerbino, Failure mechanism of normal and high-strength concrete with rice-husk ash, Cement and concrete composites 29(7) (2007) 566-574.

[23] Z.-h. He, L.-y. Li, S.-g. Du, Creep analysis of concrete containing rice husk ash, Cement and Concrete Composites 80 (2017) 190-199.

[24] N. Van Tuan, G. Ye, K. Van Breugel, A.L. Fraaij, D. Dai Bui, The study of using rice husk ash to produce ultra high performance concrete, Constr. Build. Mater. 25(4) (2011) 2030-2035.

[25] V.-T.-A. Van, C. Rößler, D.-D. Bui, H.-M. Ludwig, Rice husk ash as both pozzolanic admixture and internal curing agent in ultra-high performance concrete, Cement and Concrete Composites 53 (2014) 270-278.

[26] L. SIMCOA, ordinary Portland cement https://www.simcoa.com.au/ (2021).

[27] C. BGC-Cement, Grounded blast furnace slag, https://bgccement.com.au/ (2021).

[28] L. Xetex Industries Pvt, Microsilica, https://www.xetex.in/ (2021).

[29] Superplasticiser-Sika, https://aus.sika.com/ (2021).

[30] L. Sobute New Materials Co., Steel-fiber, http://sobute.company.weiku.com/ (2021).

[31] F. Shi, S. Yin, T.M. Pham, R. Tuladhar, H. Hao, Pullout and flexural performance of silane groups and hydrophilic groups grafted polypropylene fibre reinforced UHPC, Construction and Building Materials 277 (2021) 122335.

[32] C. Cook Industrial Minerals, Silica sand, https://cimonline.com.au/mineral-suppliers/. (2021).

[33] T.T. Tran, T.M. Pham, H. Hao, Experimental and analytical investigation on flexural behaviour of ambient cured geopolymer concrete beams reinforced with steel fibers, Eng. Struct. 200 (2019) 109707.

[34] Saloni, Parveen, T.M. Pham, Y.Y. Lim, M. Malekzadeh, Effect of pre-treatment methods of crumb rubber on strength, permeability and acid attack resistance of rubberised geopolymer concrete, Journal of Building Engineering 41 (2021) 102448.

[35] Y. Hao, H. Hao, G.P. Jiang, Y. Zhou, Experimental confirmation of some factors influencing dynamic concrete compressive strengths in high-speed impact tests, Cement and Concrete Research 52 (2013) 63-70.

[36] AS1012.9, Methods for testing concrete, Australian Standard (1986).

[37] T.M. Pham, W. Chen, A.M. Khan, H. Hao, M. Elchalakani, T.M. Tran, Dynamic compressive properties of lightweight rubberized concrete, Construction and Building Materials 238 (2020) 117705.

[38] U.S. Lindholm, Some experiments with the split hopkinson pressure bar∗, Journal of the Mechanics and Physics of Solids 12(5) (1964) 317-335.

[39] Y. Lu, Q. Li, Appraisal of pulse-shaping technique in split Hopkinson pressure bar tests for brittle materials, International Journal of Protective Structures 1(3) (2010) 363-390.

[40] T.M. Pham, M. Elchalakani, H. Hao, J. Lai, S. Ameduri, T.M. Tran, Durability characteristics of lightweight rubberized concrete, Constr. Build. Mater. 224 (2019) 584-599.

[41] M. Hassan, K. Wille, Experimental impact analysis on ultra-high performance concrete (UHPC) for achieving stress equilibrium (SE) and constant strain rate (CSR) in Split Hopkinson pressure bar (SHPB) using pulse shaping technique, Constr. Build. Mater. 144 (2017) 747-757.

[42] Y. Guo, G. Gao, L. Jing, V. Shim, Response of high-strength concrete to dynamic compressive loading, Int. J. Impact Eng. 108 (2017) 114-135.

[43] D.L. Grote, S.W. Park, M. Zhou, Dynamic behavior of concrete at high strain rates and pressures: I. experimental characterization, Int. J. Impact Eng. 25(9) (2001) 869-886.

[44] Y. Su, J. Li, C. Wu, P. Wu, Z.-X. Li, Effects of steel fibres on dynamic strength of UHPC, Construction and Building Materials 114 (2016) 708-718.

[45] R.J. Thomas, A.D. Sorensen, Review of strain rate effects for UHPC in tension, Construction and Building Materials 153 (2017) 846-856.

[46] ASTM-C1856, Standard practice for fabricating and testing specimens of ultra-high performance concrete, 2017.

[47] M. Schmidt, E. Fehling, Ultra-high-performance concrete: research, development and application in Europe, ACI Special publication 228 (2005) 51-78.

[48] J. Lee, T. Lee, Durability and engineering performance evaluation of CaO content and ratio of binary blended concrete containing ground granulated blast-furnace slag, Applied Sciences 10(7) (2020) 2504.

[49] R. Yu, P. Spiesz, H.J.H. Brouwers, Development of an eco-friendly Ultra-High Performance Concrete (UHPC) with efficient cement and mineral admixtures uses, Cement and Concrete Composites 55 (2015) 383-394.

[50] Y. Shi, G. Long, C. Ma, Y. Xie, J. He, Design and preparation of ultra-high performance concrete with low environmental impact, J. Clean Prod. 214 (2019) 633-643.

[51] Y. Su, J. Li, C. Wu, P. Wu, Z.-X. Li, Influences of nano-particles on dynamic strength of ultra-high performance concrete, Composites Part B: Engineering 91 (2016) 595-609.

[52] L.J. Malvar, J.E. Crawford, Dynamic increase factors for concrete, (1998).

[53] T. Lok, P. Zhao, Impact response of steel fiber-reinforced concrete using a split Hopkinson pressure bar, Journal of Materials in Civil Engineering 16(1) (2004) 54-59.

[54] H. Wei, A. Zhou, T. Liu, D. Zou, H. Jian, Dynamic and environmental performance of eco-friendly ultra-high performance concrete containing waste cathode ray tube glass as a substitution of river sand, Resources, Conservation and Recycling 162 (2020) 105021.

[55] M. Hassan, K. Wille, Comparative experimental investigations on the compressive impact behavior of fiber-reinforced ultra high-performance concretes using split Hopkinson pressure bar, Constr. Build. Mater. 191 (2018) 398-410.

[56] L.K. Turner, F.G. Collins, Carbon dioxide equivalent (CO2-e) emissions: A comparison between geopolymer and OPC cement concrete, Constr. Build. Mater. 43 (2013) 125-130.

[57] M.F. Alnahhal, U.J. Alengaram, M.Z. Jumaat, F. Abutaha, M.A. Alqedra, R.R. Nayaka, Assessment on engineering properties and CO2 emissions of recycled aggregate concrete incorporating waste products as supplements to Portland cement, Journal of Cleaner Production 203 (2018) 822-835.

[58] S. Park, S. Wu, Z. Liu, S. Pyo, The Role of Supplementary Cementitious Materials (SCMs) in Ultra High Performance Concrete (UHPC): A Review, Materials 14(6) (2021) 1472.